

Article

Impact-Driven Penetration of Multi-Strength Fiber Concrete Pyramid-Prismatic Piles

Isabai Bekbasarov ¹, Nurzhan Shanshabayev ^{2,*}  and Yerlan Atenov ¹ ¹ Geotechnical Testing Laboratory, Dulary University, 60, Tole bi, Taraz 080000, Kazakhstan² Department of Construction and Production of Materials, Institute of Water Management and Environmental Engineering, Dulary University, Campus 6.2, 28, Satpayev, Taraz 080000, Kazakhstan

* Correspondence: nucho91@mail.ru; Tel.: +7-707-226-05-91

Abstract: The article focuses on studying the impact-driven penetration of multi-strength fibroconcrete pyramid-prismatic piles. The research object includes multi-strength pyramid-prismatic piles with varying types of reinforcement and different levels of concrete compressive strength. The aim of the study is to experimentally investigate the enhancement of pile impact resistance through the differentiated selection of concrete strength based on the dynamic stresses in the pile shaft caused by impact forces. As a result of the experimental studies on the piles, it was found that the difference in energy costs for driving them does not exceed 3.7–4.1%, proving the insignificant influence of the type of reinforcement and fiber concrete strength on the energy expenditure during driving. At the same time, it was established that the type of reinforcement and the type of fiber significantly affect the strength and impact-resistant properties of the pile shaft, ensuring defect-free driving. For example, the defectiveness (e.g., chips, cracks, potholes, spalling) of the head of the steel fiber concrete (SFC) pile reaches 57.5%, while for the polypropylene fiber concrete (PFC) pile it does not exceed 5.2%, demonstrating the advantages of using polypropylene fiber under impact conditions.

Keywords: driven pile; polystrength pile; fiberglass; reinforcement; fiber-reinforced concrete; static tests; compressive load; deformation; dynamic tests; strength



Citation: Bekbasarov, I.; Shanshabayev, N.; Atenov, Y. Impact-Driven Penetration of Multi-Strength Fiber Concrete Pyramid-Prismatic Piles. *Buildings* **2024**, *14*, 3595. <https://doi.org/10.3390/buildings14113595>

Academic Editor: Antonio Caggiano

Received: 5 October 2024

Revised: 6 November 2024

Accepted: 8 November 2024

Published: 12 November 2024



Copyright: © 2024 by the authors. Licensee MDPI, Basel, Switzerland. This article is an open access article distributed under the terms and conditions of the Creative Commons Attribution (CC BY) license (<https://creativecommons.org/licenses/by/4.0/>).

1. Introduction

Currently, driven pile foundations are widely used at construction sites in Kazakhstan with complex engineering and geological conditions. The use of these foundations is motivated by their reliability, durability, and cost-effectiveness. It is known that replacing strip foundations with pile foundations can reduce the volume of earthworks by 50–70%, the consumption of reinforced concrete by 30% or more, labor intensity by 25%, and the estimated cost by 30% [1]. Pile production, and consequently, the construction of pile foundations, can be carried out year-round without slowing the pace of work, even in winter conditions.

However, despite these advantages, pile foundations have certain drawbacks. Among these are pile damage and failure to reach the design depth during driving. Experience with pile foundations shows that when driven into soils of medium and high strength, up to 35% of reinforced concrete piles are damaged and fail to reach the design depth (see Figure 1). Additionally, more than 80% of these piles require the undriven portion to be cut off [2,3]. These negative phenomena increase construction costs due to higher labor intensity, additional material expenses, and extended time for completing the underground portion of structures.



Figure 1. Undriven piles of the bridge under construction over the Shu River (Zhambyl Region, Republic of Kazakhstan).

Given these circumstances, in recent years, modified alternatives to traditional piles have been proposed in pile geotechnics. These include piles made of composite concrete and combined piles, which possess higher strength properties. Below are the results of several studies dedicated to examining the features of their fabrication, driving, and performance under load.

Piles made from composite concrete refer to those constructed using regular concrete but reinforced with fibers, such as steel or non-steel fibers (glass, basalt, polypropylene, polymer, asbestos, etc.). In construction, these concretes are commonly referred to as fibro concrete. Research findings presented in studies [4–8] indicate that fibro concrete is significantly more effective than conventional concrete, offering five times greater impact resistance, twice the crack resistance, 20–50% higher compressive strength, and 30–40% higher modulus of elasticity. Highly effective alkali-activated concrete (HP-AAC) is also known for use in the manufacture of concrete structures. This material is environmentally friendly, cement-free, and can replace conventional concrete and reduce CO₂ emissions [9].

Several studies [10–13] report substantial improvements in crack resistance and strength of fibro concrete piles made with steel fibers. Steel fibers are recommended as a replacement for traditional steel reinforcement in piles. Rodov G.S. et al. [14] suggested producing the head section of driven piles, 350 mm in height, from steel fiber-reinforced concrete without the use of traditional transverse reinforcement grids, to ensure defect-free driving. Experiments have shown that the impact resistance of steel fiber-reinforced concrete samples is 3.7–9.3 times higher than that of unreinforced concrete and 2–5 times higher than that of conventional reinforced concrete. Furthermore, the static compressive strength of steel fiber-reinforced concrete is 1.08–1.27 times greater than that of unreinforced concrete. The authors note that using piles with steel fiber-reinforced concrete heads reduces material losses in both concrete and reinforcement, increases the efficiency of pile-driving operations, and optimizes the use of pile-driving equipment. The high effectiveness of fibro concrete and its significant role in enhancing pile impact resistance are also noted in studies [15–21].

Among combined piles, the most common types are piles made from polymer pipes reinforced with thin fibers and piles composed of pipes filled with reinforced concrete mixtures [22–26].

Anandakumar R. [27] presents the results of impact tests conducted on 15 models of tubular (hollow) piles reinforced with basalt fiber (BFRP). The tests involved impact driving of the piles using a 78.5 kg striker dropped from a height of 1.20 m. Based on the results, it was determined that the reinforcement of piles with basalt fiber provides sufficient strength to withstand impact loads. According to the author, the greater rigidity of BFRP fibers allowed the piles to endure higher impact forces and reduced shaft deflection due to impact loads compared to conventional piles. Modernized piles using BFRP withstood 150–250% more impact loads than control piles.

In another study [28], researchers presented laboratory test results on FRP piles in sandy soil, focusing on their response to vertical and lateral loads. The tests were conducted in a specialized pressure chamber using models of CFRP piles (polymer piles reinforced with carbon fiber) and GFRP piles (polymer piles reinforced with glass fiber). The pile models, filled with concrete, were 300 mm in length, with diameters of 12.5 mm and 20 mm, and a wall thickness of 1.25 mm. The chamber pressure was set at 100 and 250 kPa. It was found that under a vertical load of 2 kN, the settlement of the GFRP pile was 8 mm, which was 1.21 times greater than that of the CFRP pile (6.6 mm). Under the same load, doubling the chamber pressure led to a 1.66-fold increase in the settlement of the CFRP pile. Thus, the CFRP pile demonstrated better resistance to vertical loads compared to the GFRP pile.

The revised text maintains the technical nature and detailed explanations required for a scientific or engineering report while being more accessible to readers. However, tests on the pile models under lateral load showed the opposite trend. The resistance force of the CFRP pile was found to be 11% lower than that of the GFRP pile. An increase in pile diameter by 1.6 times resulted in a 1.5-fold increase in lateral resistance.

In the study [29], the authors examined the behavior of piles made from thin-walled pipes reinforced with polymer fibers (FRP) and filled with concrete. The test models had a diameter of 168 mm, a wall thickness of 7.8 mm, and a length of 1.5 m. A steel tubular pile model with similar dimensions, but a thinner wall (6.35 mm), was used as the control model. The pile models were driven into sandy soil to the same depth, after which their cavities were filled with self-compacting concrete (SCC). No defects were observed on the surface of the piles after driving. It was established that under static compressive load, the bearing capacity of both the test models and the control model were comparable (120 kN and 125 kN, respectively). Under lateral load, however, the resistance force of the FRP pile model was 20 kN, 49% lower than that of the steel pile model (35 kN). The lower lateral resistance of the combined piles indicates their reduced bending stiffness, which, according to the researchers, could be improved by using stiffer fibers for pile reinforcement.

Several types of combined FRP piles were field-tested in Port Elizabeth, USA [30]. The study included the following piles:

- PPI pile (length $L = 19.8$ m, diameter $d = 38.7$ cm, made from recycled plastic reinforced with steel rods);
- SEAPILE pile (length $L = 20$ m, diameter $d = 42.5$ cm, made from recycled plastic reinforced with glass fiber reinforcement);
- Lancaster Composite pile (length $L = 18.8$ m, diameter $d = 41.9$ cm, consisting of a hollow fiberglass tube filled with expanding concrete and featuring an anti-corrosion coating);
- American Ecoboard pile (solid polyethylene pile, length $L = 11.8$ m, diameter $d = 41.9$ cm).

It was found that the Lancaster Composite and SEAPILE piles, which include glass fibers and fiberglass in their materials, exhibited fewer defects during driving and showed greater bearing capacity under compressive loads. These advantages over traditional piles and other piles used in the study suggest that these types are suitable for deep foundation construction, particularly in coastal areas and aggressive soils.

Thus, the analysis above shows that both fibro concrete piles and combined piles demonstrate strong impact resistance, which depends on factors such as the material, dimensions, reinforcing elements, and other relevant characteristics.

However, despite these advantages, it can be argued that the application of these piles is not fully efficient. This inefficiency arises from the fact that most of them are designed with uniform strength along the entire length of the shaft (with the exception of piles with fibro concrete heads). The uniform strength throughout the pile shaft negatively affects their efficiency due to the following factors.

It is well known that during pile driving, the maximum compressive stresses occur in the head (upper) section, while the lowest stresses are in the lower section. As a result, in most cases, the head of the pile is damaged during driving, while the middle and lower sections are rarely or less frequently affected (see Figure 1). This is logical since the material strength of driven piles is typically uniform along their entire length. With this approach to

pile shaft formation, the material strength in the middle and lower sections of the piles is underutilized (both during driving and operation), while the strength in the upper (head) section proves to be insufficient. Therefore, unlike traditional piles, it is advisable to use multi-strength piles composed of three sections with varying strengths, arranged according to the pattern of dynamic stress distribution during driving [3].

Based on this, in recent years, the authors have conducted comprehensive research to develop manufacturing technologies and study the behavior of multi-strength piles under both driving and static load conditions [31]. This paper presents the results of studies evaluating the impact-driven drivability of multi-strength fibro concrete pyramidal-prismatic piles. The pyramidal-prismatic piles, proposed by the authors [32], offer several significant advantages over traditional prismatic and pyramidal piles [33–36]. Therefore, transforming them into multi-strength piles and investigating them in this new, modified form is a relevant endeavor.

In the initial phase of the research, the static and impact resistance characteristics of fibro concrete pile specimens were studied, and the results are detailed in [37]. These findings form the basis for designing multi-strength fibro concrete pyramidal-prismatic piles with various reinforcement configurations and differing concrete strengths along the pile shaft.

2. Characteristics of the Pile Models, Equipment, and Research Methodology

The pile models (hereafter referred to as piles) were made from solid monolithic reinforced concrete with a uniform cross-section and continuous length. The geometric scale for the pile modeling was set at 1:3. The length of the pyramidal section of the piles was 556 mm, and the cross-sectional dimensions of the upper part of the pyramidal section were 10.0×10.0 cm (Figure 2). The slope of the side faces of the pyramidal section relative to the vertical was 0.01.

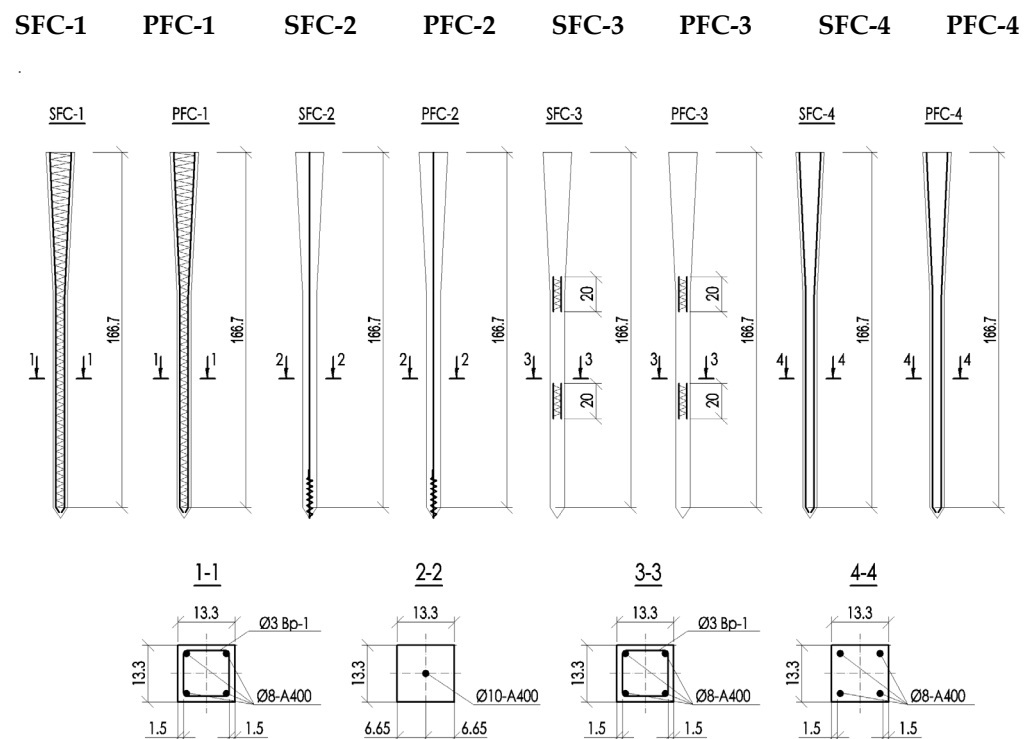


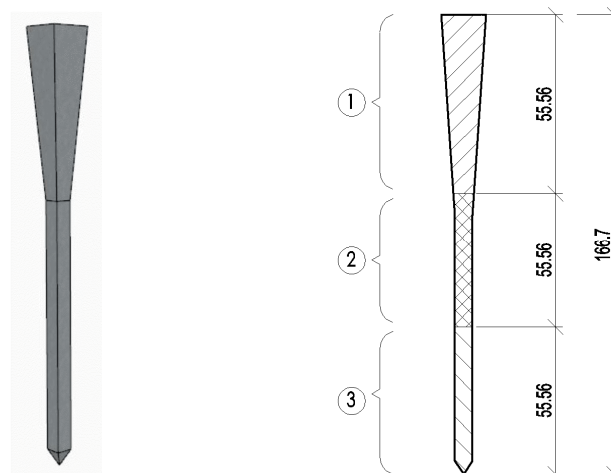
Figure 2. Pile reinforcement scheme.

For testing, piles were made using two types of fiber concrete (steel fiber-reinforced concrete—SFC—and polypropylene fiber-reinforced concrete—PFC) and constructed with the following four reinforcement methods:

1. SFC-1: Fibro concrete pile made with DRAMIX 3D steel fibers, non-prestressed longitudinal reinforcement, and transverse reinforcement along the shaft;
2. PFC-1: Fibro concrete pile made with polypropylene fibers, non-prestressed longitudinal reinforcement, and transverse reinforcement along the shaft;
3. SFC-2: Fibro concrete pile made with DRAMIX 3D steel fibers and non-prestressed central reinforcement;
4. PFC-2: Fibro concrete pile made with polypropylene fibers and non-prestressed central reinforcement;
5. SFC-3: Fibro concrete pile made with DRAMIX 3D steel fibers, featuring localized frame reinforcement at the boundary between concrete layers of different strengths, and non-prestressed longitudinal and transverse reinforcement;
6. PFC-3: Fibro concrete pile made with polypropylene fibers, featuring localized frame reinforcement at the boundary between concrete layers of different strengths, and non-prestressed longitudinal and transverse reinforcement;
7. SFC-4: Fibro concrete pile made with DRAMIX 3D steel fibers, non-prestressed longitudinal reinforcement, without transverse reinforcement along the shaft;
8. PFC-4: Fibro concrete pile made with polypropylene fibers, non-prestressed longitudinal reinforcement, without transverse reinforcement along the shaft.

The framework reinforcement arrangement and principles for the piles were designed in accordance with the standard requirements [38]. For longitudinal reinforcement, steel bars with a periodic profile, 6 mm in diameter, of class A400 were used. The longitudinal bars of the piles (for piles SFC-1, PFC-1, SFC-4, and PFC-4) were assembled into a framework by spirally winding steel wire, 3 mm in diameter, which served as the transverse reinforcement. The transverse reinforcement of class Vr-1 was tied to the longitudinal bars using wire of class 1.0-O-C (Figure 2).

These prepared reinforcement frameworks were placed into wooden molds of the corresponding shape. Each mold was pre-divided into three equal-length sections using temporary transverse partitions to facilitate the production of piles with different concrete strengths. The first section included the upper part of the pile, namely the pyramidal portion of the shaft; the second section corresponded to the middle prismatic part of the shaft; and the third section represented the lower prismatic part of the shaft and the pile tip (Figure 3). Each section of the piles was 55.56 mm in length. The first section was filled with concrete mix corresponding to class B20 for compressive strength, the second section with mix corresponding to class B15, and the third section with mix corresponding to class B12.5.



(a) General view of the pile (b) Diagram of dividing the pile shaft into equal sections

Figure 3. Type and diagram of pile with sections.

This principle of pile manufacturing is adopted to meet the experimental goal of producing piles with sections of varying strength along the shaft. This approach ensures optimal strength distribution during pile driving, where the maximum compressive stresses are concentrated at the head and the minimum stresses occur at the lower part.

The inner surface of the molds was treated with technical oil to ensure the defect-free removal of the finished piles. The placement of the reinforcement frameworks in the molds was performed while considering the formation of a protective concrete layer of the required thickness.

Fine-grained concrete was used for pile casting, with the selection of concrete components made in accordance with standard [38]. To produce piles with varying concrete strengths, separate preparation of the concrete mix was carried out. During the preparation process, steel fibers (DRAMIX 3D) and polypropylene fibers were added to the mix in dosed amounts, with a reinforcement ratio ($\mu = 1\%$) [37]. The prepared fiber-reinforced concrete mix was then placed into the molds, which already contained the reinforcement frameworks. Each section of the mold was filled with a concrete mix of the corresponding strength.

After the molds were filled, the temporary partitions that divided the mold into separate sections were removed. Vibrational loading was applied to the molds using the "Grohot KP-109" (manufactured in the Russian Federation) to ensure proper compaction of the concrete mixture. Once the concrete had gained initial strength, the piles were extracted from the molds and stored until they reached the required strength.

The appearance of the pile molds and fragments of their filling with fiber-reinforced concrete are shown in Figure 4.



Figure 4. Appearance of pile models and segments filled with fiber-reinforced concrete. Pile Models: (a) SFC-1 and PFC-1; (b) SFC-2 and PFC-2; (c) SFC-3 and PFC-3; (d) SFC-4 and PFC-4; (e) filled with concrete.

The strength of the concrete in the piles was assessed after the curing period through the testing of control samples made from the fiber-reinforced concrete mix collected during

the pile manufacturing process. These control samples, measuring $100 \times 100 \times 100$ mm, underwent compressive strength testing (Figure 5) using a hydraulic press P-125, produced in Russia. The tests were carried out in accordance with the standards outlined in [38].

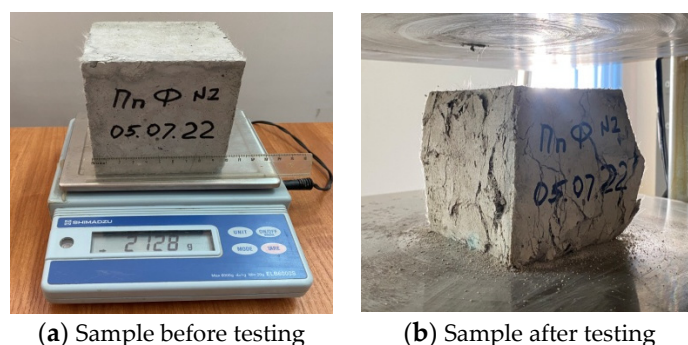


Figure 5. Control samples before and after testing.

The results of testing control samples of fiber-reinforced concrete for compressive strength confirmed that they meet the required strength for their respective concrete classes: B20 in the first (upper) section of the piles, B15 in the second (middle) section, and B12.5 in the third (lower) section, aligning with the research objectives.

Impact driving of the piles was conducted at the testing ground located on the premises of the Southern Kazakhstan branch of KazNIISA JSC. The experimental site, measuring 6.0×3.0 m in plan and 3.0 m deep, was composed of sandy loam. Site preparation included layer-by-layer placement and uniform compaction of the soil from the bottom of the previously excavated pit. The physical and mechanical characteristics of the soil were determined using the penetration method with the PSG MG-4 device (Table 1).

Table 1. Physical and mechanical characteristics of the soil at the experimental site.

Characteristics	Humidity, W, %	Density, ρ , kg/m ³	Moisture at the Pour Point, W _T , %	Moisture at the Rolling Edge, W _P , %	Plasticity Number, I _p	Maximum Penetration Resistance, P _{max} , MPa	Specific Adhesion, c, MPa	Internal Friction Angle, φ , grade	Deformation Modulus, E, MPa
The values	2.97–4.89	1680–1750	25.01–25.58	16.95–17.30	6.75–6.85	1.50–1.65	0.017–0.018	16.9–17.5	16.5–20.4

To drive and test the pile models, special experimental equipment has been developed and manufactured (Figure 6). The parameters, principles, and sequence of operations using this equipment are described in detail in the study [39].

The driving of piles into the ground was carried out through impact driving with a consistent energy level for each blow. A hammer weighing 60 kg was dropped onto the pile head from a height of 0.5 m (see Figure 7). To protect the pile head from destruction, a removable metal cap was used. A wooden board, 30 mm thick and covering the entire area of the upper end of the pile, was installed as a shock absorber between the cap and the pile.

The pile-driving process was accompanied by a count of the number of blows, assessing the energy expenditure of the hammer during installation. The piles were driven to an equal depth, measuring between 145.0 and 145.5 cm, with a maximum deviation of just 0.34%. Additionally, during the driving process, monitoring was conducted to observe the appearance and progression of defects on the surface of the piles as the number of blows increased.

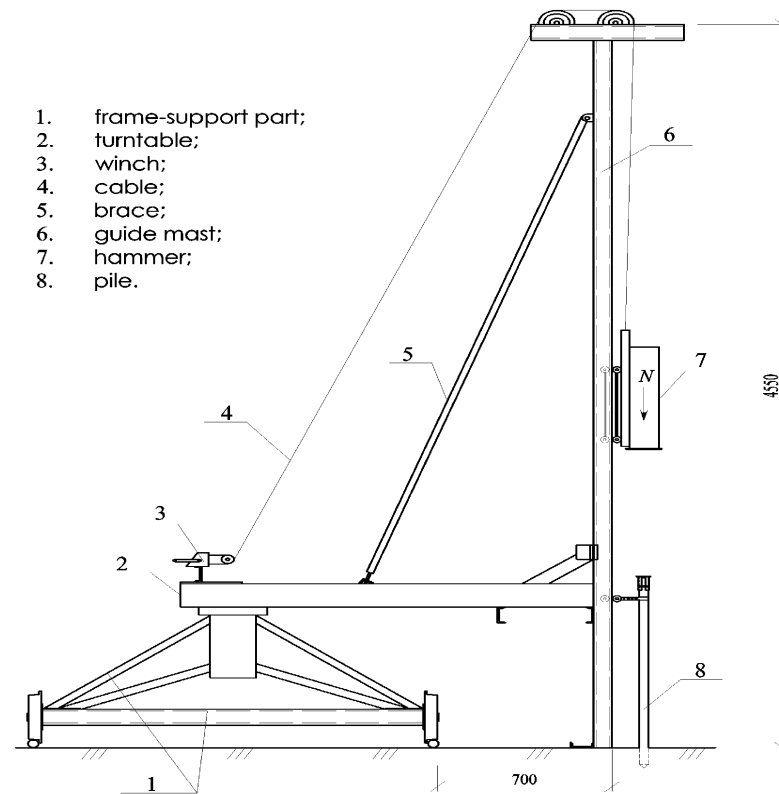


Figure 6. Diagram of equipment for pile driving in field conditions.



(a)



(b)

Figure 7. Fragments of pile driving (a) and instrumental diagnostics of piles (b).

According to the regulatory guidelines [40], the criteria for acceptable defectiveness of the piles were established as follows, specifically regarding the condition of their head section post-driving:

- The deviation of the pile's end surface from the horizontal should not exceed 5° ;
- The width of any concrete spalling around the perimeter of the pile's cross-section should not exceed 50 mm;
- Wedge-shaped spalls at the corners should not exceed 35 mm;

- The length of wedge-shaped spalls should be at least 30 mm above the pile's embedded surface in the soil.

After the piles were driven, an instrumental diagnosis of the driving depth and localization of defects in the pile shaft was performed (see Figure 7) using the PDS-MG4 device (produced by LLC "SKB Stroypribor," Chelyabinsk, Russia). The diagnostic work was carried out following the requirements of the PNST 804-2022 "Piles. Seismoacoustic Method for Controlling Length and Continuity" [41].

3. Research Results

Information on the energy costs of driving in the form of a histogram is shown in Figure 8.

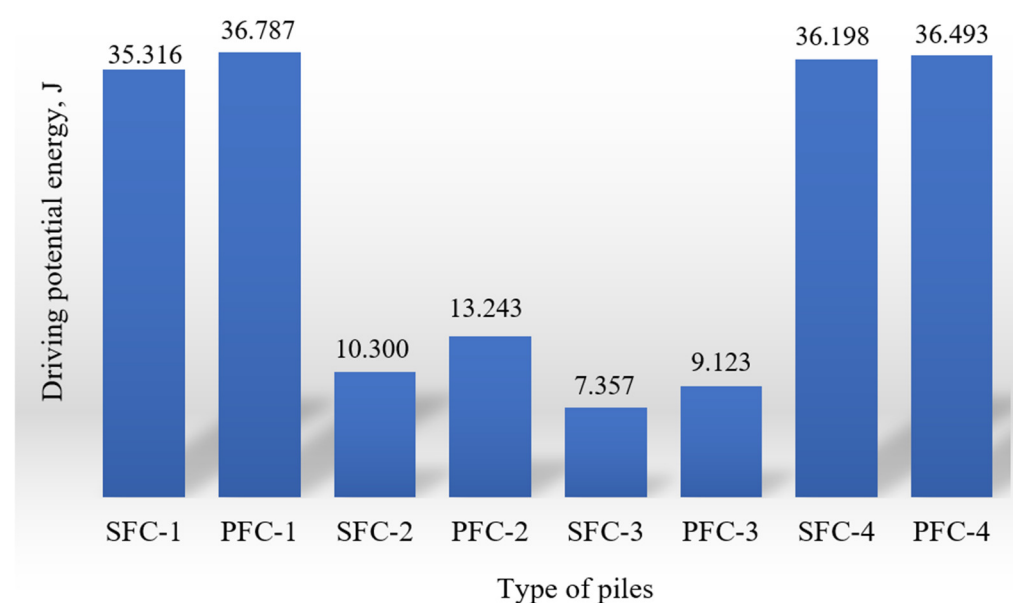


Figure 8. Histogram of pile driving.

The assessment of the drivability and energy efficiency of the fiber-reinforced pyramidal-prismatic piles was conducted based on the following indicators:

- The number of hammer blows spent on driving the pile model;
- The specific energy intensity of driving a pile model E_v , taken as the ratio of the total potential energy of the impact of the impactor spent on driving the model to the volume of its immersed part in the ground (see Figure 8);
- The coefficient of relative energy intensity of driving a pile model K_e , taken as the ratio of the total potential energy of the impactor's impacts spent on driving the experimental model pile to a similar energy parameter of the control model of the pile.

The findings from the study reveal several key features of the driving process for the test piles:

- Full embedding to the required depth was achieved for piles SFC-1, PFC-1, SFC-4, and PFC-4;
- Piles SFC-2, PFC-2, SFC-3, and PFC-3 experienced significant damage, preventing them from being driven to the desired depth (see Figure 8);
- Both the potential energy and the specific energy consumption during the driving of piles SFC-1, PFC-1, SFC-4, and PFC-4 were closely aligned, with differences not exceeding 4.1% and 3.7%, respectively.

During the driving of piles SFC-2 and PFC-2, initial defects appeared as horizontal cracks with a width of up to 0.5 mm at the junction of the pyramidal and prismatic sections of the piles after 16–17 impacts of the hammer. Further increases in the number of impacts

led to the widening of these cracks and a reduction of the piles' penetration into the ground, ultimately resulting in their stoppage. When the number of impacts reached 35–45, the width of the cracks in the piles exceeded 2 mm, leading to a loss of integrity in the pile shaft, separating it into distinct pyramidal and prismatic parts (see Figure 9c,d).



Figure 9. Driven piles and their defects: (a) SFC-1; (b) PFC-1; (c) SFC-2; (d) PFC-2; (e) SFC-3; (f) PFC-3; (g) SFC-4; (h) PFC-4.

Inspection of the piles after their failure revealed that the head section of the pile had no significant defects, apart from minor chips around the perimeter with widths of 5–8 mm. This indicates that the fiber-reinforced concrete sufficiently protected the integrity of the head section. However, the emergence of defects that resulted in the failure of piles SFC-2 and PFC-2 suggests that the reinforcement of their shafts with fibers and central longitudinal reinforcement does not adequately safeguard against structural failure.

For piles SFC-3 and PFC-3, the first (hairline) cracks, with a width of up to 0.25 mm, were observed after 10–12 impacts at the locations of the local reinforcement cages. As the number of impacts increased, the width of these cracks grew by 0.5 mm with every subsequent five impacts. Complete failure of the piles occurred after 25–30 impacts (see Figure 9e,f), with small sections of concrete chipping off at the local reinforcement areas. The shafts of these piles were divided into three distinct parts: the upper pyramidal section above the first local reinforcement area; the middle prismatic section between the reinforcement areas; and the lower prismatic section below the second local area. An

inspection of the piles after failure showed that the head section exhibited no significant defects other than minor chips around the perimeter, with widths not exceeding 7 mm.

The failure of piles SFC-3 and PFC-3, which did not achieve the required embedding depth, highlights that reinforcement of the pile shafts with fibers and local reinforcement at the boundaries of sections with varying strengths do not ensure the integrity of the piles, even though the defects in the head sections remained within the criteria for acceptable defect levels [39].

The driving of piles SFC-1 and SFC-4 was accompanied by damage to the concrete of the reinforcement in their head sections. At the end of the driving process, after the piles reached the required depth, the following defects were identified (see Figure 9a,g):

- Partial exposure and bending of longitudinal and transverse reinforcement;
- Concrete chips around the perimeter of the pile heads exceeding 60–80 mm;
- Significant wedge-shaped chips at the corners of the pile heads with depths greater than 90 mm.

The nature, size, and extent of these defects do not fully comply with the criteria for acceptable defect levels in piles [39]. Piles SFC-1 and PFC-4 underwent acoustic inspection using the PDS-MG4 device (see Figure 10a,c), revealing micro cracks at a depth of 46 cm from the ground surface in the shaft of pile FPP-1. Similar micro cracks were detected in the shaft of pile SFC-4 at a depth of 51 cm from the surface. These findings indicate that the identified defects developed in the middle section of the piles, where the concrete strength was rated at B15.

Thus, piles SFC-1 and SFC-4, made from DRAMIX 3D steel fiber-reinforced concrete with peripheral longitudinal reinforcement, exhibited low impact resistance regardless of the presence or absence of transverse reinforcement. Such reinforced piles may be suitable for ensuring a rigid connection of the pile heads to a monolithic raft, as in such cases, the defective section of the pile head is subject to forced destruction, exposing the reinforcement. As a means of enhancing the impact resistance of the examined piles, it is recommended to use higher-strength concrete for the upper and middle sections during their manufacture.

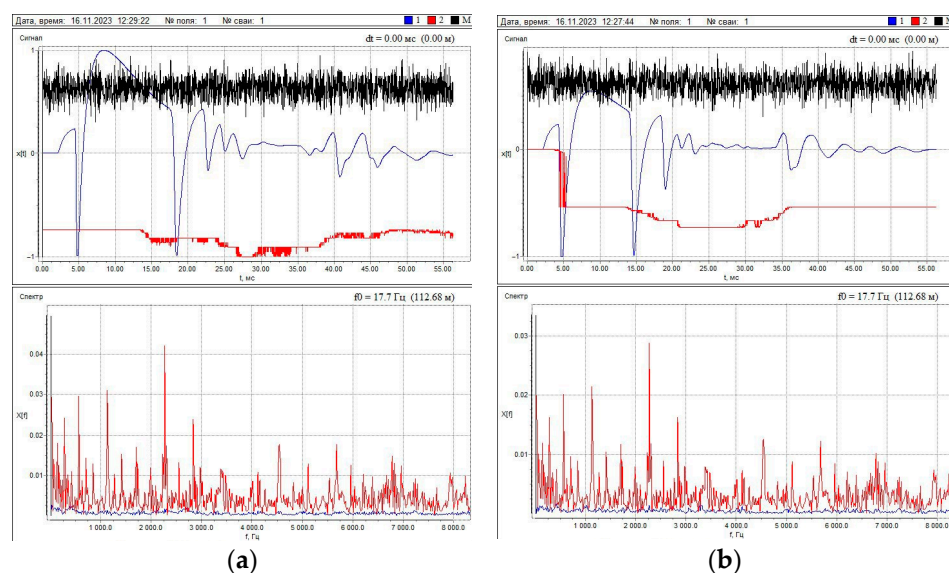


Figure 10. Cont.

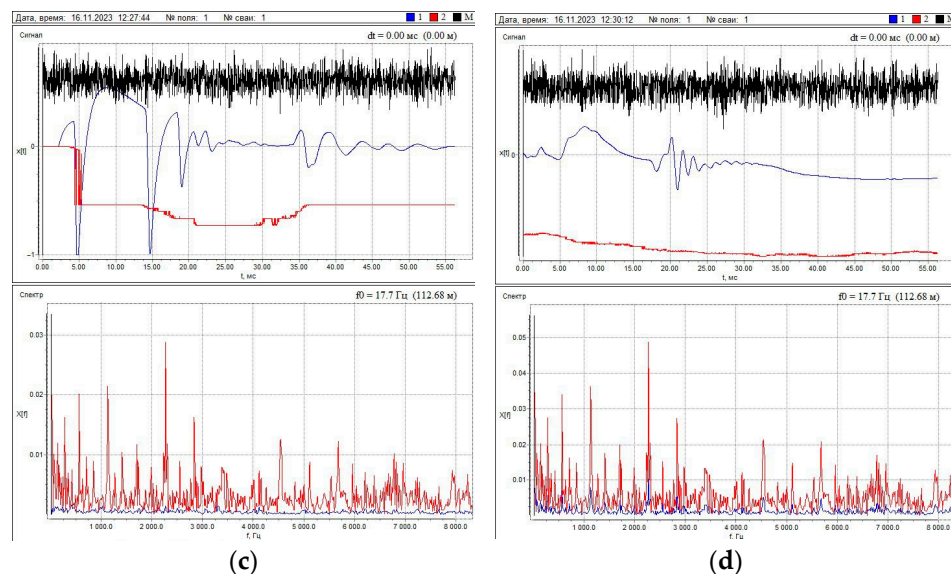


Figure 10. Results of testing piles using the acoustic method: (a) SFC-1; (b) PFC-1; (c) SFC-4; (d) PFC-4.

In contrast to all the experimental piles, including SFC-1 and SFC-4, piles PFC-1 and PFC-4, constructed from fiber-reinforced concrete with polypropylene fibers, were driven to the required depth without significant defects. The inspection revealed only minor concrete chips in the head section, measuring up to 5–7 mm. Acoustic inspections of these piles showed no micro defects (see Figure 10b,d). The condition of these piles meets the criteria for acceptable defect levels [39]. Therefore, piles reinforced with polypropylene fibers and featuring peripheral reinforcement, with or without transverse reinforcement, can be classified as impact-resistant foundation structures. From an economic perspective, pile PFC-4, which lacks traditional transverse reinforcement, is the more advantageous option among these piles.

4. Conclusions

Based on the results of the experimental studies presented, the following key conclusions can be drawn:

- Influence of Reinforcement Type and Material Strength: the type of reinforcement and the strength of the material in fibrous, multi-strength pyramidal-prismatic piles do not affect the energy expenditure required for their installation to the required depth;
- Impact of Central and Local Reinforcement: Fibrous, multi-strength piles with central reinforcement and similar piles with local reinforcement at the boundaries of sections with varying concrete strength do not possess impact resistance. In these structures, both the type of reinforcement and the kind of fibers do not influence the piles' impact resistance. These piles can be used in weak or loose, uncompacted soils, employing the method of static pushing for their installation;
- Performance of Steel Fiber-Reinforced Piles: Multi-strength piles made of concrete with DRAMIX 3D steel fibers, featuring longitudinal peripheral and transverse reinforcement of the shaft, as well as similar piles without transverse reinforcement, exhibit low impact resistance. The impact resistance of such piles can be improved by utilizing higher-strength concrete for their construction;
- Performance of Polypropylene Fiber-Reinforced Piles: Multi-strength piles made from concrete with polypropylene fibers, which have longitudinal peripheral and transverse reinforcement, as well as similar piles without transverse reinforcement, demonstrate high impact resistance. It is economically advantageous to use piles without transverse reinforcement, which can be effectively employed in dense and medium-density soils;
- Effect of Fiber Type on Impact Resistance: In the pile structures referenced in points 3 and 4, the type of fiber does influence the impact resistance of the piles. The use of

polypropylene fibers in the construction of piles helps preserve their material integrity during driving, preventing damage;

- Influence of Reinforcement Type and Material Strength: the type of reinforcement and material strength in fibrous, multi-strength pyramidal-prismatic piles do not significantly affect the energy expenditure required for their installation to the desired depth;
- Impact of Central and Local Reinforcement: Fibrous, multi-strength piles with central reinforcement, as well as those with local reinforcement at the boundaries of sections with varying concrete strengths, do not exhibit notable impact resistance. In these structures, neither the type of reinforcement nor the type of fibers affects their impact resistance. Such piles are suitable for installation in weak or loose, uncompacted soils, using the method of static pushing;
- Performance of Steel Fiber-Reinforced Piles: Multi-strength piles made of concrete with DRAMIX 3D steel fibers, incorporating longitudinal peripheral and transverse shaft reinforcement—or lacking transverse reinforcement—show low impact resistance. Enhancing the impact resistance of these piles is possible by using higher-strength concrete;
- Performance of Polypropylene Fiber-Reinforced Piles: Multi-strength piles made from concrete reinforced with polypropylene fibers, with both longitudinal peripheral and transverse reinforcement or without transverse reinforcement, demonstrate high impact resistance. For economic efficiency, using piles without transverse reinforcement is advantageous, and they can be effectively used in dense and medium-density soils;
- Effect of Fiber Type on Impact Resistance: In the pile structures described in Sections 3 and 4, the type of fiber does affect impact resistance. The use of polypropylene fibers helps maintain the structural integrity of piles during driving, preventing damage.

These findings underline the significance of material selection and reinforcement strategies in optimizing the performance of fibrous piles within various soil conditions, ultimately guiding engineers toward more resilient and cost-effective foundation solutions.

Author Contributions: Conceptualization, I.B. and N.S.; methodology, I.B. and N.S.; formal analysis, I.B., N.S. and Y.A.; writing—original draft, I.B., N.S. and Y.A. All authors have read and agreed to the published version of the manuscript.

Funding: This research has been funded by the Science Committee of the Ministry of Education and Science of the Republic of Kazakhstan (Grant No. AP13268763). Any opinions, findings, conclusions, or recommendations expressed in this material are those of the researchers and do not necessarily reflect the views of the Ministry of Education and Science of the Republic of Kazakhstan.

Data Availability Statement: The original contributions presented in the study are included in the article, further inquiries can be directed to the corresponding author.

Acknowledgments: The authors grateful to Science Committee of the Ministry of Education and Science of the Republic of Kazakhstan.

Conflicts of Interest: The authors declare no conflicts of interest.

References

1. Pukhareenko, Y.; Panteleev, D.; Zhavoronkov, M. Influence of fiber type and matrix composition on adhesive strength in fiber reinforced concreting. *Russ. Automob. Highw. Int. J.* **2022**, *19*, 436–445. [[CrossRef](#)]
2. Klyuev, S.V.; Klyuev, A.V.; Vatin, N.I. Fiber concrete for the construction industry. *Mag. Civ. Eng.* **2018**, *84*, 41–47. [[CrossRef](#)]
3. Bekbasarov, I.; Isakov, G. Driven-in poly-strength reinforced concrete piles and a new pile cap design. *Nauka I Tekhnika* **2015**, *2*, 47–54.
4. Levkovich, T.I.; Mevlidinov, Z.A.; Fedin, N.A. Application of fibro concrete mixture at construction of bases and coatings automobile roads. *Russ. J. Transp. Eng.* **2020**, *3*, 45–56. [[CrossRef](#)]
5. Nazhuev, M.P.; Khalyushev, A.K.; Tkach, P.S.; Efimov, I.I.; Sanin, I.S.; Kurbanov, N.S.; Orlov, M.G. Efficiency of using various types of fiber and coarse aggregate in vibro centrifuged concrete. *Eurasian Sci. J.* **2020**, *2*, 1–10. Available online: <https://esj.today/PDF/45SAVN220.pdf> (accessed on 28 August 2024).
6. Ivlev, M.A.; Strugovets, I.B.; Nedoseko, I.V. Comparative assessment of the bearing capacity, crack resistance and deformability of lintels with standard and dispersed reinforcement. *Izv. KGASU* **2012**, *22*, 117–123.

7. Kabdushev, A.; Delikesheva, D.; Korgasbekov, D.; Manapbayev, B.; Kalmakhanova, M. Identifying the influence of basalt fiber reinforcement on the deformation and strength characteristics of cement stone. *East.-Eur. J. Enterp. Technol.* **2023**, *5*, 58–65. [CrossRef]
8. Kabdushev, A.; Agzamov, F.; Manapbayev, B.; Delikesheva, D.; Korgasbekov, D. Research and development of cements with differential properties for completing gas wells. *News Natl. Acad. Sci. Repub. Kazakhstan Ser. Geol. Tech. Sci.* **2023**, *4*, 97–108. [CrossRef]
9. Torkan, S.; Farzin, K.; Neda, A.; Doo-Yeol, Y. Machine-learning methods for estimating compressive strength of high-performance alkali-activated concrete. *Eng. Appl. Artif. Intell.* **2024**, *136 Pt B*, 109053.
10. Fang, O.; Jianjing, Z.; Xiaoning, D.; Jianwei, H.; Junwei, B.; Lin, D. Analysis of Load Capacity Behaviors of Steel Fiber Reinforced Concrete Piles Through Model Tests. *J. Shanghai Jiao Tong Univ.* **2016**, *50*, 364–369. Available online: <https://xuebao.sjtu.edu.cn/EN/Y2016/V50/I03/364> (accessed on 4 September 2024).
11. Buyle-Bodin, F.; Madhkhani, M. Seismic behaviour of steel fibre reinforced concrete piles. *Mat. Struct.* **2002**, *35*, 402–407. [CrossRef]
12. Sokolova, V.F.; Kurbatov, L.G.; Borovskikh, I.N.; Rabinovich, F.N.; Sterin, V.S. On the effectiveness of the use of steel-fiber-reinforced concrete in reinforced concrete pile structures. *Bases Found. Soil Mech.* **1985**, *6*, 4–7. [CrossRef]
13. Tulebekova, S.; Zhang, D.; Kim, J.; Lee, D.; Ju, H. Analytical Study of Using Fiber-Reinforced Concrete Pile Foundation for Renewable Energy Storage. In Proceedings of the 2018 Structures Congress (Structures18) Songdo Convensia, Incheon, Republic of Korea, 27–31 August 2018.
14. Rodov, G.; Kurbatov, L.; Kuprianov, V.; Khazanov, M. Driven Piles with Reinforced Concrete Shaft and Steel-fiber-Reinforced Concrete Head. In Proceedings of the Workshop on Quality Improvement of Zero Cycle, Moscow, Russia, 28 June 1979; pp. 54–62. (In Russian)
15. Møller Andersen, M.E.; Poulsen, P.N.; Olesen, J.F.; Hoang, L.C. Strength-Based Material Layout Optimization of Solid Reinforced Concrete. *Comput. Struct.* **2023**, *276*, 106941. [CrossRef]
16. Ozden, G.; Akdag, C.T. Lateral load response of steel fiber reinforced concrete model piles in cohesionless soil. *Constr. Build. Mater.* **2009**, *23*, 785–794. [CrossRef]
17. El-Sayed, A.; Roshdy, M.; Noaman Emar, A. A Study of Vertical Load Capacity of Carbon Fiber Concrete Piles Reinforced with Geosynthetics. *Int. J. Adv. Eng. Manag. Sci.* **2023**, *9*, 9. [CrossRef]
18. Tan, C.; Jiang, X.; Qiang, X.; Fan, M. Flexural Performance of Carbon Fiber-Reinforced Polymer Prestressed Spun High-Strength Concrete Pile. *Appl. Sci.* **2024**, *14*, 7170. [CrossRef]
19. Akdag, C.T.; Özden, G. Soil-Pile Interaction of Reinforced Concrete Piles with Steel Fibers. In Proceedings of the 3rd International Soil-Structure Interaction Symposium, Izmir, Turkey, 18–20 October 2017.
20. Barrett, J.W.; Luke, J. Prendergast Empirical Shaft Resistance of Driven Piles Penetrating Weak Rock. *Rock Mech. Rock Eng.* **2020**, *53*, 5531–5543. [CrossRef]
21. Bao, X.; Shi, J.; Chen, G.; Li, Y.; Hu, J.; Cui, H. Laboratory Tests and Numerical Simulation of the Thermal–Mechanical Response of a Fiber-Reinforced Phase Change Concrete Pile. *Appl. Sci.* **2023**, *13*, 11853. [CrossRef]
22. Zyka, K.; Mohajerani, A. Composite piles: A review. *Constr. Build. Mater.* **2016**, *107*, 394–410. [CrossRef]
23. Boyarintsev, A.V. Polymer and Composite Piles. International and Russian Experience. *Soil Mech. Found. Eng.* **2020**, *57*, 415–421. [CrossRef]
24. Venkatesan, G.; Arul Murugan, C.; Isac, S.J.; Jerome Nithin Gladson, G. Experimental investigation on load carrying capacity of hollow and composite pile materials in layered soil. *Mater. Today Proc.* **2022**, *65*, 3951–3958. [CrossRef]
25. Sabri, M.M.S.; Vatin, N.I.; Nurmukhametov, R.R.; Ponomarev, A.B.; Galushko, M.M. Vertical Fiberglass Micropiles as Soil-Reinforcing Elements. *Materials* **2022**, *15*, 2592. [CrossRef] [PubMed]
26. Farhangi, V.; Karakouzian, M. Effect of Fiber Reinforced Polymer Tubes Filled with Recycled Materials and Concrete on Structural Capacity of Pile Foundations. *Appl. Sci.* **2020**, *10*, 1554. [CrossRef]
27. Anandakumar, R.; Selvamony, C.; Seeni, A.; Singh, S. Bright. Performance of basalt fiber reinforced polymer (BFRP) composites retrofitted RCC piles subjected to impact loads. *Int. J. Appl. Eng. Res.* **2015**, *10*, 13339–13352.
28. Lu, Y.; Abuel-Naga, H.; Shaia, H.A.; Shang, Z. Preliminary Study on the Behaviour of Fibre-Reinforced Polymer Piles in Sandy Soils. *Buildings* **2022**, *12*, 1144. [CrossRef]
29. Nehdi, M.; Sakr, M.; El Naggar, M.-H. Toe-Driven Tapered Fiber-Reinforced Polymer Self-Consolidating Concrete Composite Piles: New High-Performance Technology for Deep Foundations. *Geotech. Test. J.* **2008**, *31*, 3. [CrossRef]
30. Juran, I.; Komornik, U. *Behavior of Fiber-Reinforced Polymer (FRP) Composite Piles Under Vertical Loads*; Report No. FHWA-HRT-04-107; U.S. Department of Transportation, Federal Highway Administration: Washington, DC, USA, 2006; p. 97.
31. Shanshabayev, N.; Bekbasarov, I.; Atenov, Y. Study of the strength properties of various types of fiber-reinforced concrete under static compressive load for the production of driven piles. *Mech. Technol.* **2024**, *2*, 175–189. [CrossRef]
32. Bekbasarov, I.I.; Shanshabayev, N.A. Precast Reinforced Concrete Pile. Patent 4521 RK, 29 November 2019.
33. Bekbasarov, I.; Nikitenko, M.; Shanshabayev, N.; Atenov, Y.; Moldamuratov, Z. Tapered-prismatic pile: Driving energy consumption and bearing capacity. *News Natl. Acad. Sci. Repub. Kazakhstan Ser. Geol. Tech. Sci.* **2021**, *6*, 53–63. [CrossRef]
34. Bekbasarov, I.; Shanshabayev, N. Driving Features of Tapered-Prismatic Piles and Their Resistance to Static Loads. *Acta Montan. Slovaca* **2022**, *4*, 55–65. [CrossRef]

35. Bekbasarov, I.; Atenov, Y. Equations Used to Calculate Vertical Bearing Capacity of Driven Piles with Shaft Broadenings. *Period. Polytech. Civ. Eng.* **2020**, *64*, 1235–1243. [[CrossRef](#)]
36. Bekbasarov, I.; Shanshabayev, N. Impact Dipping Pyramidal-Prismatic Piles and their Resistance to Pressure and Horizontal Load. *Period. Polytech. Civ. Eng.* **2021**, *65*, 909–917. [[CrossRef](#)]
37. Bekbasarov, I.; Shanshabayev, N.; Atenov, Y. Strength Properties of Various Types of Fiber-Reinforced Concrete for Production of Driven Piles. *Buildings* **2023**, *13*, 1733. [[CrossRef](#)]
38. GOST 26633-2015; Concrete Is Heavy and Fine-Grained. Specifications. Interstate Standard: Moscow, Russia, 2019; p. 15.
39. Bekbasarov, I.; Baitemirov, M.; Atenov, Y.; Shanshabayev, N. About experimental equipment for driving and testing large-scale model piles in the field. *Mech. Technol.* **2019**, *4*, 134–141.
40. SP RK 5.01-101-2013; Earthworks, Bases and Foundations. Code of Rules of the Republic of Kazakhstan. JSC KazNIISA: Astana, Kazakhstan, 2015; p. 108.
41. PNST 804-2022; Piles. Seismoacoustic Method for Monitoring Length and Continuity. Preliminary National Standard of the Russian Federation. Interstate Standard: Moscow, Russia, 2023; p. 24.

Disclaimer/Publisher’s Note: The statements, opinions and data contained in all publications are solely those of the individual author(s) and contributor(s) and not of MDPI and/or the editor(s). MDPI and/or the editor(s) disclaim responsibility for any injury to people or property resulting from any ideas, methods, instructions or products referred to in the content.